The 2009 IEEE/RSJ International Conference on
Intelligent Robots and Systems
October 11-15, 2009 St. Louis, USA

Multi-Sensor Fusion for Reduced Uncertainty in Autonomous Mobile Robot Docking and Recharging

Ren C. Luo[1], Chung T. Liao[12], Shih C. Lin[1]

[1] *Intelligent Robotic and Automation Laboratory*
Department of Electrical Engineering
National Taiwan University

[2]*Department of Electronic Engineering*
Wu-Feng Institute of Technology

renluo@ntu.edu.tw, ctliao@ ira.ee.ntu.edu.tw , sclin@ ira.ee.ntu.edu.tw

***Abstract*—The power management system for autonomous mobile robots is an important issue for keeping robots in their long-time functionality. Recharging is necessary before the power of the robot has exhausted. In this paper, we propose a multi-sensor fusing method using intensity and range data fusion with covariance intersection approach to locate the robot pose while performing the docking for recharging. An artificial landmark is employed as a visual cue on a docking station in order to recognize the location by using inverse perspective projection. At the same time, the range data acquired by laser range finder are modeled as multiple line segments which are the hypothetical walls in the environment. Then the geometrical relationship between the robot and the docking station is estimated much more precise by using covariance intersection approach. We have demonstrated the success of the proposed algorithms through experimental results.**

I. Introduction

With the increasingly research on mobile robot in recently decades, the role of the robot will be more important in the current and future world. Mobile robots are being designed to interact increasingly with human environment, working around humans on a daily basis. The robot systems will be widely employed in many applications, for example, factory automation, dangerous environments, office, hospitals, surgery, entertainment, space exploration, farmland, military, security system, and so on. In this paper, we describe our fully designed and developed mobile robot for indoor services [1]. With this purpose, the robot should be provided with multiple sensors for adapting the change of the environments in order to take the duty of services. Efficient communication between the robot and its outside world is also necessary. In addition, the robot must be capable of long-term autonomy. Energy power is of great concern, and without it the robot will become immobilized and useless. How to navigate the robot towards the recharging station and dock into the station are important issues for the long-term functionality of robot.

The first work on robot recharging is made by Grey Walters [3]. They developed the first autonomous recharging mobile robots and employed light to find a hut, which contains a light beacon and a battery recharger. Roufas [4] used four IR LED emitters and one IR receiver to implement the docking. Their method can allow 6 degree of error. In [5], the robot approaches the recharging station using the map and makes contact with specially designed battery recharging system. Some systems are using vision-based method to implement docking [6~9]. The robot designed by Silverman [8] consists of an immobile docking station and the docking mechanism mounted on the robot. Vision and laser ranger-finder are used in two phase mode to find the docking station. The docking station is designed with 2 degree of freedom to tolerate the docking error.

Intensity image acquired by camera is passive perceptual sensor data and always hard to obtain the pose of the robot with respective to the docking station. Although the laser range sensor is active perceptual and perfect in estimating the distance between robot and the object, it is difficult to find the target in the environment. Our research aims to combine the two kinds of sensor by using covariance intersection to locate the docking station in the environment in order to locate the pose with respective to the docking station. This paper is organized as follows: In Section II, we introduce the system configuration of our service robot including the docking station and robot docking mechanism. We present the image and range data model in section III and IV respectively. Session V describes the fusion algorithm with covariance intersection. Section VI presents the experimental results. Section VII presents brief concluding remarks.

II. Robot System Configuration

A. Robot Hardware Architecture

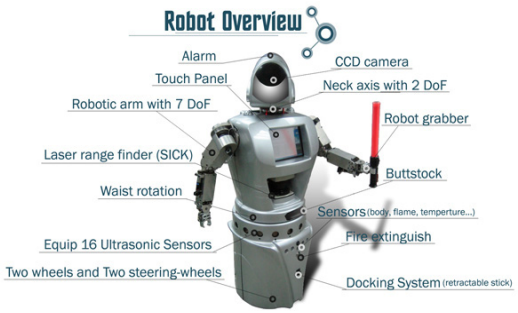

Fig. 1. Hardware structure of service robot, developed in IRA Lab. at NTU.

The mobile robot we developed for services is shown in

Fig. 2. The robot is designed for security patrol in office building, warehouses home services and developed by our laboratory. The robot is equipped with main controller (employed by Pentium-IV with 512M RAM), sensory circuits, single camera, laser range finder, power management system, and two 7 D.O.F. arms. The structure of the hardware is shown in Fig.1.

B. Software Architecture

The software architecture is shown in Fig. 2. Task behaviors are executed by the kernel which is the central part of control and intelligence. The kernel can communicate with all the sub-systems through the IPC (Inter-Process Communication).

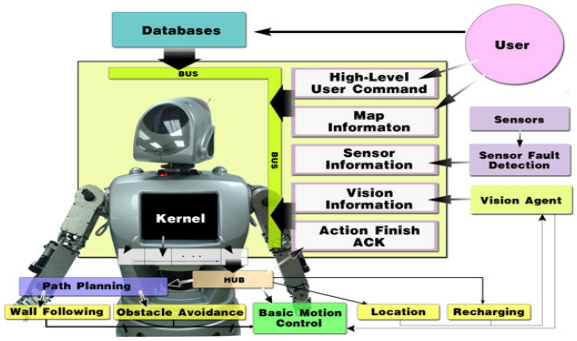

Fig. 2. Software architecture of service robot.

C. Docking Station and Robot Docking Mechanism

Unlike the other approached [4~9], our robot equips a charger inside the robot. This makes the docking and recharging station be simple in its architecture and easily implemented. The docking and recharging station can be mounted everywhere in the working environment. When robot about to run out its battery power, it will decide to recharge and find the nearest station to dock and charge.

The docking station and robot docking mechanism are shown in Fig. 3(a) and (b) respectively. The system diagram is shown in the left side of Fig. 5. It consists of MPU (Microprocessor unit), IR and DPDT (Double pole double throw) replay. The MPU acts as the main controller and communicates to robot through infrared rays. Only under the successful docking and encrypted communication between robot and docking station, the controller turns on the AC power and begins the charging procedures. This encrypted communication confirms the safety of the charging system. The diagram of the communication is demonstrated in Fig, 5.

The robot docking mechanism is shown in Fig. 3(b). They are mounted in front of the robot. The recharging adapter is located inside the robot and extends out through servo control when docking is proceeding. A tolerable entry offset and angle are allowed when robot is in the docking process.

Fig. 3. (a) Docking station. (b) The robot docking mechanism which is under servo control.

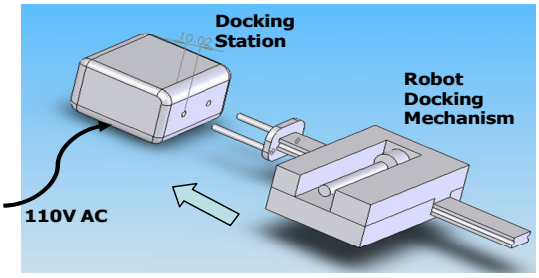

Fig. 4. The motion of the robot docking mechanism.

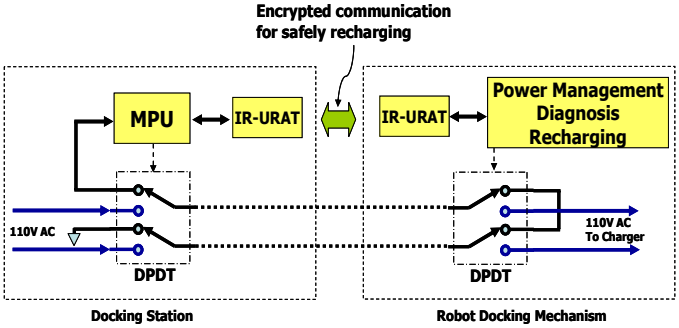

Fig. 5. Recharge system diagram for the docking station and robot.

III. IMAGE MODEL

Fig.6 illustrates the geometrical relationship of camera and ranger finder. The color camera is mounted on top of the ranger finder. An extra servo-controlled device is to perform the tilt function of the range finder. The plane of range data is produced by swinging the LRF (Laser range finder). Color image is captured by the camera. The information such as range data and image data are gathered and computed in the PC mounted on robot and the process of the data fusion with range and image is also running on the PC.

A. Coordinate System

There are two kinds of coordinates in our robot. One is the image coordinate system (ICS), and the other is the range coordinate system (RCS). Fig. 6 shows the geometric relationship of ICS and RCS. Vector $\vec{T}$ is the translation vector from RCS to ICS. The z-axis of ICS is parallel to the z-axis of RCS. Thus there is no rotation in the coordinate transformation from RCS to ICS. The parameters x_T, y_T, z_T of the translation vector $\vec{T}$ are constant and can be measured in advance.

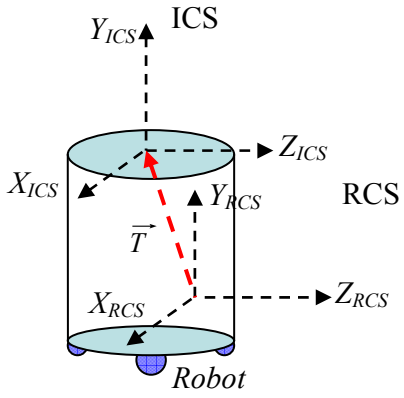

Fig. 6. The geometric relationship of ICS and RCS in the robot.

We use the 4×4 homogeneous matrix T_{ICS}^{RCS} to transform RCS to ICS. The transformation matrix T_{ICS}^{RCS} is defined as:

$$T_{ICS}^{RCS} = \begin{bmatrix} 1 & 0 & 0 & x_T \\ 0 & 1 & 0 & y_T \\ 0 & 0 & 1 & z_T \\ 0 & 0 & 0 & 1 \end{bmatrix} \tag{1}$$

Then,

$$(x,y,z,1)_{ICS}^{RCS} = T_{ICS}^{RCS}(x,y,z,1)_{RCS}^{T} \tag{2}$$

B. Camera Model

Define the camera model is:

$$I = AX, \tag{3}$$

where I is column vector $(u,v,t)^T$ and represents the homogeneous coordinates in the image plane. X is the column vector $(x,y,z,1)^T$ and represents the homogeneous coordinates in the world coordinate system (the same as ICS). The A is 3×4 matrix mapping three-dimensional world points to two-dimensional image points and is denoted as the parameters of camera calibration. The image coordinates $(U,V)^T$ is thus obtained by

$$U = \frac{u}{t},\ V = \frac{v}{t}, \tag{4}$$

For any world point (x,y,z), we can obtain the coordinates in the image plane by

$$u = A_1X,\ v = A_2X,\ t = A_3X, \tag{5}$$

where A_1 is the row vector in A. Expand the inner products and rewrite $u - Ut = 0$ and $v - Vt = 0$,

$$\begin{cases} xA_{11} + yA_{12} + zA_{13} + A_{14} - UxA_{31} - UyA_{32} - UzA_{33} - UA_{34} = 0 \\ xA_{21} + yA_{22} + zA_{23} + A_{24} - VxA_{31} - VyA_{32} - VzA_{33} - VA_{34} = 0 \end{cases} \tag{6}$$

The overall scaling of A is irrelevant, due to the homogeneous formulation, A_{34} may be arbitrarily set to 1. The afore mentioned equations can be written in matrix form:

$$\begin{bmatrix} x^1 & y^1 & z^1 & 1 & 0 & 0 & 0 & 0 & -U^1x^1 & -U^1y^1 & -U^1z^1 \\ 0 & 0 & 0 & 0 & x^1 & y^1 & z^1 & 1 & -V^1x^1 & -V^1y^1 & -V^1z^1 \\ \vdots & & & & & & & & & & \vdots \\ 0 & 0 & 0 & 0 & x^n & y^n & z^n & 1 & -V^nx^n & -V^ny^n & -V^nz^n \end{bmatrix} \begin{bmatrix} A_{11} \\ A_{12} \\ \vdots \\ A_{33} \end{bmatrix} = \begin{bmatrix} U^1 \\ V^1 \\ \vdots \\ U^n \\ V^n \end{bmatrix} \tag{7}$$

We denote the above equation by $Y = PB$, where:

$$y = \begin{bmatrix} U^1 \\ V^1 \\ \vdots \\ U^n \\ V^n \end{bmatrix}, B = \begin{bmatrix} A_{11} \\ A_{12} \\ \vdots \\ A_{33} \end{bmatrix}, \tag{8}$$

$$P = \begin{bmatrix} x^1 & y^1 & z^1 & 1 & 0 & 0 & 0 & 0 & -U^1x^1 & -U^1y^1 & -U^1z^1 \\ 0 & 0 & 0 & 0 & x^1 & y^1 & z^1 & 1 & -V^1x^1 & -V^1y^1 & -V^1z^1 \\ \vdots & & & & & & & & & & \vdots \\ 0 & 0 & 0 & 0 & x^n & y^n & z^n & 1 & -V^nx^n & -V^ny^n & -V^nz^n \end{bmatrix} \tag{9}$$

To solve the equation for vector B, The Pseudo-Inverse Method [10] is adopted. The linear model is represented by

$$Y = PB + E, \tag{10}$$

where X is an $n\times p$ formal independent variable matrix, B is a $p\times1$ parameter matrix whose values are to be determined and E represents the difference between the prediction and the actuality. E is an $n\times1$ error matrix. To minimize the error, the error term is:

$$E^TE = (Y-PB)^T(Y-PB) = Y^TY - B^TP^TY - Y^TPB + B^TP^TPB$$
$$= Y^TY - 2B^TP^TY + B^TP^TPB \tag{11}$$

Now differentiate, setting the derivative to 0 yields

$$P^TPB - P^TY = 0 \tag{12}$$

And thus

$$B = P^*Y = ((P^TP)^{-1}P^T)Y \tag{13}$$

Where P^* is called the pseudo-inverse of P

IV. Range Data Model

We consider that the model of laser range finder is a sphere as shown in Fig. 7, where α, β, d are pan-angle, tilt-angle and range data.

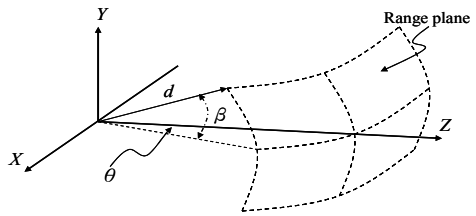

Fig. 7. The model of laser range finder.

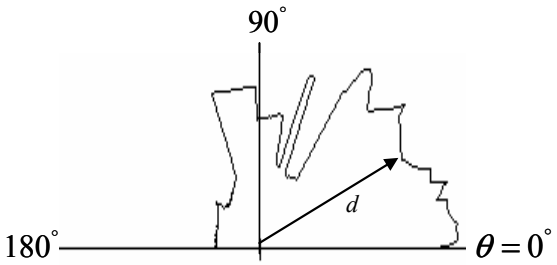

Fig. 8. An example of range image scanned in a line.

The range data d and pan angle α_R is measured by LRF, and β_R is the tilt angle controlled by the extra servo-controlled device. In Fig. 7, R represents the range plane composed of range data. In Fig. 8, it shows the range image which is scanned in a wall line. The laser range model is composed of many spherical arcs and one of spherical arcs represents a range image scanned in a wall line.

A. *Cluster of Collinear Points*

A scan of range data is represented by $s = \{p_0, ..., p_n\}$, where $p_j = \{x_j, y_j\}$ represents the Cartesian coordinates and j is the acquired angle of the laser range finder. By the natural wall segment extraction, the first step is to apply an Iterative Endpoint Fit (IEPF) [10,11] on the measurements data set s. Fig. 9 shows that the IEPF will recursively split s into two subsets $s_1 = \{p_0, ..., p_j\}$ and $s_2 = \{p_j, ..., p_n\}$ until a validation criterion distance d_{max} is satisfied from point $\{p_j\}$ to the virtual line segment consisted of $\{p_0, p_n\}$. Finally the IEPF function will return to all the end points $\{p_0, p_j\}$ 、$\{p_j, p_n\}$.

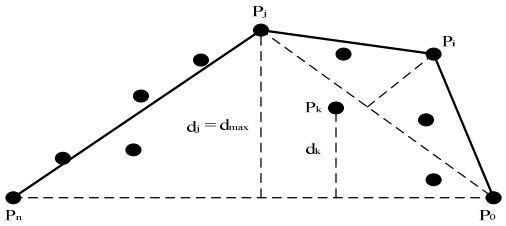

Fig. 9. The recursive split of IEPF.

B. *IEPF with Weighting*[16]

Fig. 10 (a) shows the IEPF results when the laser scans near a corner. Because the vertex of corner is beyond a distance measurement (3 meter), the IEPF will lead out three line segments. Obviously, the shortest line segment is not the true candidate. In this experiment, we modify the IEPF by adding a weighting sum. When the point number of a line segment is over than a threshold value (for example the threshold is 5), the line segment from IEPF is valid. Otherwise, the line segment is inactive. Fig. 10 (b) shows the IEPF with a weighting sum threshold.

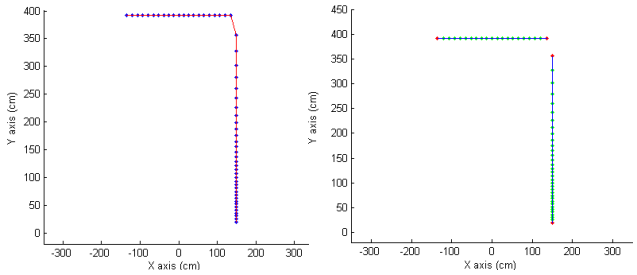

(a) (b)

Fig. 10. (a) The IEPF result without weighting, (b) and with weighting.

C. *Uncertainty Estimation from Hough Transform*

The Hough Transform is one of the popular approached to extract lines as IEPF. However in this paper, we utilize the Hough Transformation for re-sampling the co-linear points which have been clustered into groups from the Weighting IEPF.

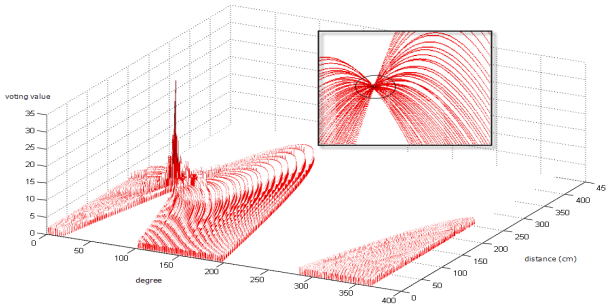

Fig. 11. The Hough Transform.

Fig. 11 shows the Hough Transform result [12, 13]. A maximum voting value indicates the most possible line feature in $\{R_{max}, \phi_{max}\}$.Nevertheless, surrounding region of $\{R_{max}, \phi_{max}\}$ also shows the uncertainty. For this reason, we can re-sample the Hough domain within the dark ellipse to estimation the mean, variance and covariance of the line feature. Fig. 12(a) shows two line segments from the weighting IEPF and Fig. 12(b) shows the line feature uncertainty within 2-deviation.

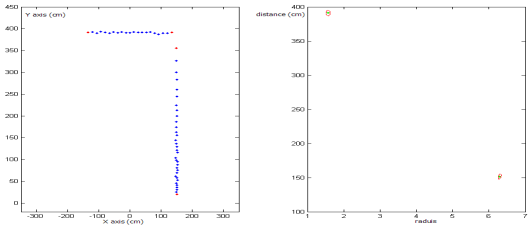
(a) (b)

Fig. 12. The estimation of line feature uncertainty.

V. Sensor Fusion With Covariance Intersection

In general, for the feature extraction from docking station, we can obtain reliable orientation information from vision system, but may get rough depth information. On the other

hand, LRF model process is in contrast with vision process, it is easy to measure the accurate distance of an extracted object, but it is hard detect and recognize the feature in the environment.

In these proposed approach, we combine the vision feature with range model feature to reduce uncertainty of detecting and recognizing the landmark of the docking station. Sensor fusion improves the measurement performance when different sensor modalities are measuring the same target. Fig. 13 shows the complementary correlation. The ellipses represent the measuring uncertainties.

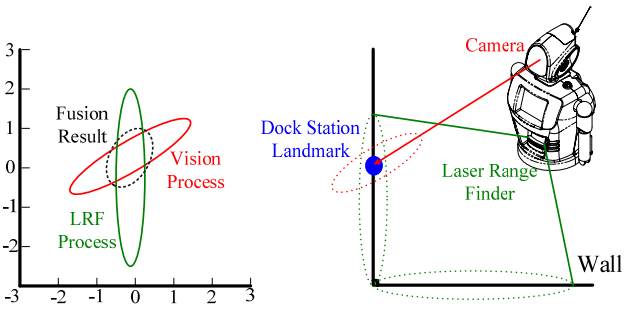

Fig. 13. Shows the complementary correlation.

Two pieces of information, μ_v and μ_l, are to be fused together to yield an output μ_o, where μ_v and μ_l are estimation from vision and laser range finder system model, and P_{vv}, P_{ll} and P_o are their covariance. The Covariance Intersection Algorithm (CI) [14] is used to fuse these. The intersection is characterized by the convex combination of the covariance, and the Covariance Intersection algorithm is:

$$P_o^{-1} = \omega P_{vv}^{-1} + (1-\omega) P_{ll}^{-1} \quad (14)$$

$$P_o^{-1}\mu_o = \omega P_{vv}^{-1}\mu_v + (1-\omega) P_{ll}^{-1}\mu_l \quad (15)$$

where $\omega \in [1, 0]$, and ω modifies the relative weights assigned to P_{vv}^{-1} and P_{ll}^{-1}. Different choices of ω can be used to optimize the covariance estimate with respect to different performance criteria such as minimizing the determinant of P_o^{-1}. The fact that this update is conservative for every ω and it can be shown using a proof by [15] which demonstrating the matrix

$$P_o - E[\tilde{\mu}_o \tilde{\mu}_o^T] \quad (16)$$

is positive semidefinite for any cross covariance P_{vl} between the two prior estimates:

The error $\tilde{\mu}_o = P_o(\omega P_v^{-1}\tilde{\mu}_v + (1-\omega)P_l^{-1}\tilde{\mu}_l)$, where $\tilde{\mu}_v$ and $\tilde{\mu}_l$ are the errors in μ_v and μ_l.

In other words, the Covariance Intersection method provides an estimate and a covariance matrix whose covariance ellipsoid encloses the intersection region. The estimate is consistent irrespective of any value of P_{vl}.

If there are more than one line feature in a laser scan, camera has to search the docking station landmark in the region of each line feature. When the vision feature has been detected in the region of corresponding line feature, the Covariance Intersection Algorithm (CI) is used to fuse these to estimate an accurate docking position. The key algorithm procedure is shown as follows:

Complementary Fusion Algorithm

Data: all line features (μ_l^i , P_{ll}^i) in a local scan

Result: To estimate of the docking position information, and update them when they are identical.

Initialize: landmark detection = False

For *all line features from each scan* **do**

- Calculate the region angle θ^i

$$P_{ll}^i = \begin{bmatrix} \sigma_x^2 & \sigma_{xy} \\ \sigma_{xy} & \sigma_y^2 \end{bmatrix}, \text{ and } \theta^i = 90^o + \frac{1}{2}\tan^{-1}\frac{2\sigma_{xy}}{\sigma_x^2 - \sigma_y^2}$$

- Trigger vision feature detection at θ^i

- Compute the vision feature μ_v^i and covariance matrix P_{vv}^i

If *vision feature has been detected* **then**

- Fuse line feature and vision feature with CI

$$P_o = \left[\ \omega P_{vv}^{-1} + (1-\omega) P_{ll}^{-1}\ \right]^{-1}$$

$$\mu_o = \omega P_o P_{vv}^{-1}\mu_v + (1-\omega) P_o P_{ll}^{-1}\mu_l$$

- landmark detection = True
- Break the for loop

Else

- Jump to the line feature next *i*

End

- landmark detection = False

End

VI. Experimental Result

The proposed data fusion algorithm using covariance intersection approach is implemented in our robot. Fig. 14 shows the docking scenario that our robot using combined intensity and range data to locate the docking station by covariance intersection. The result of fusing intensity and range data using covariance intersection is shown in Fig. 16. Range data can be extracted several line features which representing walls. Since the docking station is located against wall, there exists five line features in this range data. Thus, image data has to be processed for finding the landmark in the corresponding parts of the acquired image. When the landmark is extracted and the pose of docking station is estimated by inverse perspective projection, the covariance intersection algorithm (CI) fuses these to estimate an accurate docking pose. Fig. 17 shows that CI can reduce the uncertainty of the pose of docking station. The trajectory of robot and environment map acquired by laser ranger finder is shown in Fig. 15.

Fig. 14. An image acquired in our test trial.

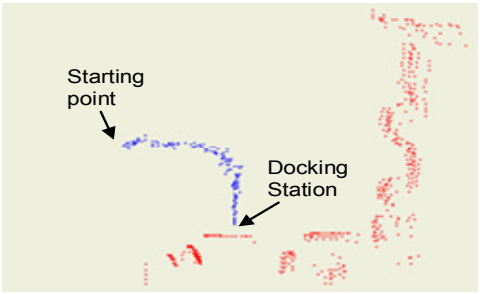

Fig. 15. The result of successive trail is shown. The blue points represent the trajectory of robot and red ones are partial environment map nearby the docking station.

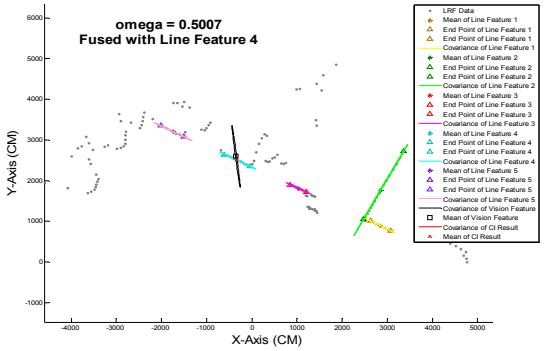

Fig. 16. The result of intensity and range data fusing with covariance intersection.

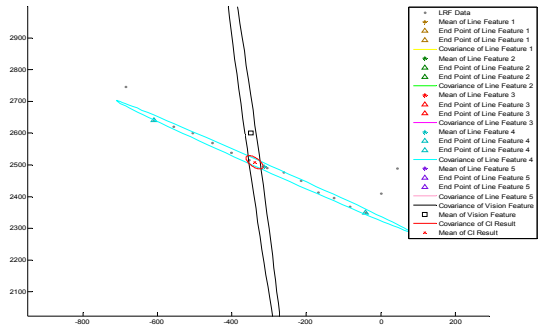

Fig. 17. The covariance intersection estimation for locating the docking station.

VII. Conclusion

Using the docking station and robot docking mechanism developed in our laboratory, the proposed data fusion with covariance intersection is implemented in our service robot. An artificial landmark is employed as a visual cue on a docking station in order to recognize the location by using inverse perspective projection. At the same time, the range data acquired by laser range finder are modeled as multiple line segments which are the hypothetical walls in the environment. Then the geometrical relationship between the robot and the docking station is estimated much more precisely by using covariance intersection approach. Our approach is superior in reducing the uncertainty than the approach which individually uses image and range data in two phase mode to achieve docking.

References

[1] R. C. Luo, K. L. Su, "A multiagent multisensor based real-time sensory control system for intelligent security robot," IEEE International Conference on Robotics and Automation, vol. 2, pp. 2394 - 2399, Sept. 2003.

[2] Y. Takahashi, I. Masuda, "A visual interface for security robots," IEEE International Workshop on Robot and Human Communication, pp. 123- 128, Sept. 1992.

[3] W. G. Walter, "The Living Brain," W. W. Norton, New York, 1953.

[4] K. Roufas, Y. Zhang, D. Duff, M. Yim," Six degree of freedom sensing for docking using IR LED emitters and receivers," The 7th Intl. Symp. On Experimental Robotics, 2000.

[5] S. Yuta, Y. Hada, "Long term activity of the autonomous robot – Proposal of a bench-mark problem for the autonomy, " I International Conference on Intelligent Robots and Systems, pp. 1871-1878, Oct. 1998.

[6] R.C. Arkin, R. R. Murphy, "Autonomous navigation in a manufacturing environment," IEEE Trans, Robot. Automat. vol. 6, pp. 445-454, Aug. 1990.

[7] B.W Minten, R.R. Murphy, J. Hyams, M. Micire, " Low-order-complexity vision-based docking," IEEE Transactions on Robotics and Automation, vol. 17, iss. 6, pp. 922-930, Dec. 2001.

[8] M.C. Silverman, D. Nies, B. Jung , G.S. Sukhatme, "Staying alive: a docking station for autonomous robot recharging," IEEE International Conference on Robotics and Automation, 2002. Proceedings. ICRA '02. , vol. 1, pp. 1050-1055, May 2002.

[9] N. Barnes, Z. Q. Liu, "Fuzzy Control for Active Perceptual Docking," The 10th IEEE International Conference on Fuzzy Systems, vol. 3, pp. 1531-1534, Dec. 2001.

[10] T.S. Michael, T. Quint, "Sphere of inuence graphs in general metric spaces, " Mathematical and Computer Modeling, pp. 45-53, 1994.

[11] G. A. Borges, M.-J. Aldon, "Line Extraction in 2D Range Images for Mobile Robotics," Journal of Intelligent and Robotic Systems, pp. 267-297, 2004.

[12] Hokuyo Automation, Scanning laser range finder for robotics, http://www.hokuyo-aut.jp/products/urg/urg.htm, 2005.

[13] S. T. Pfister, S. I. Roumeliotis, J. W. Burdick, "Weighted Line Fitting Algorithms for Mobile Robot Map Building and Efficient Data Representation," Proceedings of the IEEE International Conference on Robotics and Automation, 2003.

[14] S.J. Julier, J.K Uhlmann, "A non-divergent estimation algorithm in the presence of unknown correlations," American Control Conference, vol.4, pp.2369-2373, Jun. 1997.

[15] S. Julier and J. Uhlmann, "A nondivergent estimation algorithm in the presence of unknown correlations," American Control Conference, 1997.

[16] R.C. Luo, S. C. Lin, C. C. Lai, "Indoor autonomous mobile robot localization using natural landmark," IEEE Conference of Industrial Electronics, pp. 1626-1631, Nov. 2008.